# A novel dual enrichment strategy provides soil- and digestate-competent $N_2O$-respiring bacteria for mitigating climate forcing in agriculture

Kjell Rune Jonassen[1,2], Ida Ormåsen[1], Clara Duffner[3], Torgeir R Hvidsten[1], Åsa Frostegård[1], Lars R Bakken[1], Silas HW Vick[1*].

[1)] Faculty of Chemistry, Biotechnology and Food Science, Norwegian University of Life Sciences, Norway

[2)] VEAS WWTP, Bjerkåsholmen 125, 3470 Slemmestad, Norway.

[3)] Helmholtz Zentrum München, Deutsches Forschungszentrum für Gesundheit und Umwelt (GmbH), Germany.

* corresponding author

Journal: Water Science, or Environmental science and technology, or ISME

**Graphical abstract**

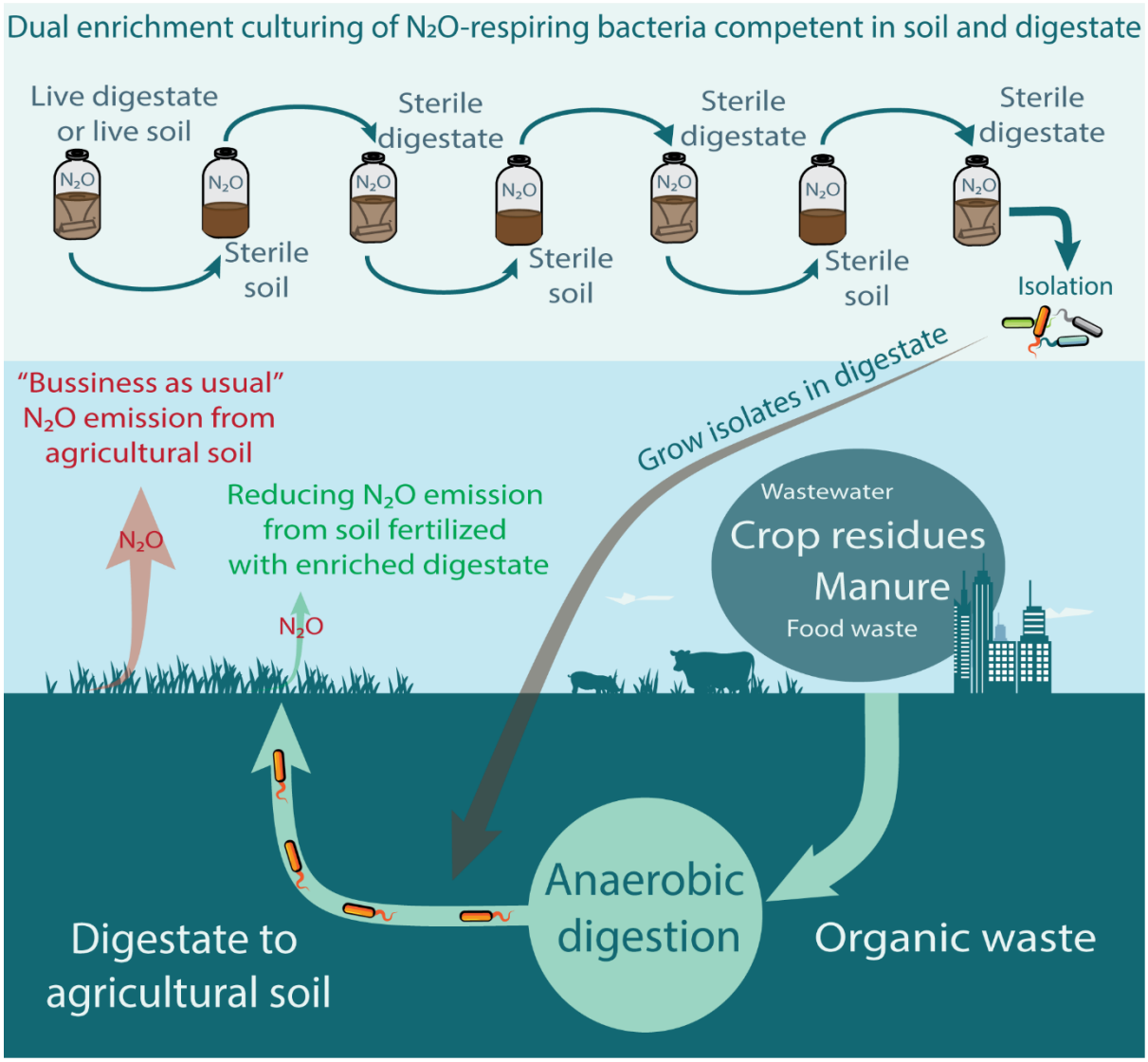

## Abstract

Manipulating soil metabolism by heavy inoculation with microbes is deemed realistic if waste from anaerobic digestion (digestate) is utilized as substrate and vector, but requires organisms that can grow both in digestate and soil (=generalist). We designed a strategy to enrich and isolate such generalist $N_2O$-respiring bacteria (NRB) in soil and digestate, to provide inoculum for reducing $N_2O$-emissions from agricultural soil. Sequential anaerobic enrichment cultures were provided with a small dose of $O_2$ and unlimited $N_2O$, alternating between sterilized digestate and soil as substrates. The cultures were monitored for gas kinetics and community composition (16SrDNA), and cluster-analysis identified generalist-OTUs which became dominant, digestate/soil-specialists which did not, and a majority that were diluted out. Several NRBs circumscribed by generalist-OTU's were isolated, genome sequenced to screen for catabolic capacity, and phenotyped, to assess their capacity as $N_2O$-sinks in soil. The two isolates *Cloacibacterium* sp., carrying only $N_2O$-reductase (Clade-II) and *Pseudomonas sp.,* with full-fledged denitrification-pathway, were both very effective $N_2O$-sinks in soil, with *Pseudomonas* sp., showing a long-lasting sink effect, suggesting better survival in soil. This avenue for utilizing waste to bioengineer the soil microbiota holds promise to effectively combat $N_2O$-emissions but could also be utilized for enhancing other metabolic functions in soil.

## Introduction

The $N_2O$-concentration in the atmosphere is increasing, largely driven by the input of reactive nitrogen species in agriculture (Davidson 2009, Thompson et al 2019). $N_2O$-emissions from farmed soils account for 52 % of the total anthropogenic emissions of $N_2O$ (Tian et al 2020) and approximately 1/3 of the climate forcing from food production (Robertson 2014). Limiting the input of reactive nitrogen to soils would be an effective mitigation measure but at the expense of lowering crop yields. This dichotomy has proven difficult to bypass, and estimates indicate only modest $N_2O$ mitigation potentials if currently available $N_2O$ abatement options were to be implemented at large scale (Winiwarter et al 2018).

In agricultural soils nitrification and denitrification are the main sources of $N_2O$ (Butterbach-Bahl et al 2013). Nitrous oxide reductase (Nos) is the only known enzyme catalyzing the reduction of $N_2O$. Nos is expressed as part of the denitrification pathway sustaining anaerobic respiration by stepwise reduction of $NO_3^- \rightarrow NO_2^- \rightarrow NO \rightarrow N_2O \rightarrow N_2$, catalyzed by the enzymes nitrate reductase (Nar), nitrite reductase (Nir), nitric oxide reductase (Nor) and nitrous oxide reductase (Nos) encoded by the genes *nar*/*nap*, *nir*, *nor* and *nosZ*, respectively (Zumft 2007). A significant share of denitrifying prokaryotes, however, are truncated, i.e. lacking genes encoding for 1 to 3 of the four enzymes (Shapleigh 2013; Graf et al 2014), and truncated denitrifying pathways may significantly affect the $N_2O$-emissions in soils under denitrifying conditions. Organisms that lack all denitrification genes other than *nosZ* are particularly interesting as they can act as net sinks for $N_2O$. The propensity of the soil community to emit $N_2O$ can be reduced by increasing the relative abundance of such $N_2O$-respiring bacteria (NRB) (Philippot et al 2011, Domeignoz-Horta et al 2016). However, as a stand-alone operation, such modification of soil microflora by inoculation would be prohibitively expensive.

We have previously demonstrated that anaerobic digestion (AD) provides a promising industrial platform for low-cost large-scale introduction of $N_2O$-reducing bacteria to soil (Jonassen et al 2021): denitrifying bacteria with a strong preference for $N_2O$ over $NO_3$ were isolated from an AD-digestate, which could be grown aerobically to high cell densities in a sterilized digestate, providing a cheap inoculum for reducing $N_2O$-emission from soil. The isolated organisms did not include NRB (bacteria with only *nosZ*), however, and it was evident that the organisms were not well adapted for activity and survival in soil. Here we present a new approach to obtain more ideal isolates by a deliberate attempt to enrich (and isolate) organisms that can grow both in digestate and soil. Conceptually the $N_2O$-reducing organisms within a community can be divided into three categories according to their ability to grow/survive in digestates and soil: *digestate specialists* (***D***) with a competitive advantage in digestate, *soil specialists* (***S***) with a competitive advantage in soil, and *generalists* (***G***) organisms capable of growth in both environments, but plausibly at lower growth rates in both substrates relative to the two specialists. We hypothesized that we could enrich ***G*** by sequential enrichment culturing, alternating between soil and digestate as substrate (coined *dual enrichment*), and explored this with a logistic growth model for the competition between three organisms, assigning hypothetical growth and death rates. The model revealed that the selective pressure could be modulated by the duration of each enrichment and the fraction of enriched material transferred from one enrichment to the next, and predicted that a reasonably competitive *generalist* would reach dominance after a limited number of repeated passages.

Using this theoretical framework, we designed an enrichment strategy whereby a microbial community, originating from digestate or soil, was passaged through a series of enrichment cultures alternating between gamma sterilized soil (ϒ-soil) and autoclave sterilized digestate (AC-digestate) (**Fig. 1**). We anticipated that *generalists* would gradually increase in abundance throughout the enrichment series and that organisms that are non-competitive in either substrates would be washed out due to the repeated dilution each transfer represented. Strong specialists would likely reappear when reintroduced in their preferred environment, and thus be easily identifiable. By means of this novel enrichment strategy along with targeted isolation of $N_2O$ respiring isolates, genome sequencing and physiological experiments designed to unravel the isolates´ denitrifying regulatory phenotypes, we provide insight into the targeted enrichment of generalist type organisms and their performance as $N_2O$ mitigating inoculants when vectored by digestate to agricultural soil.

## Materials and methods

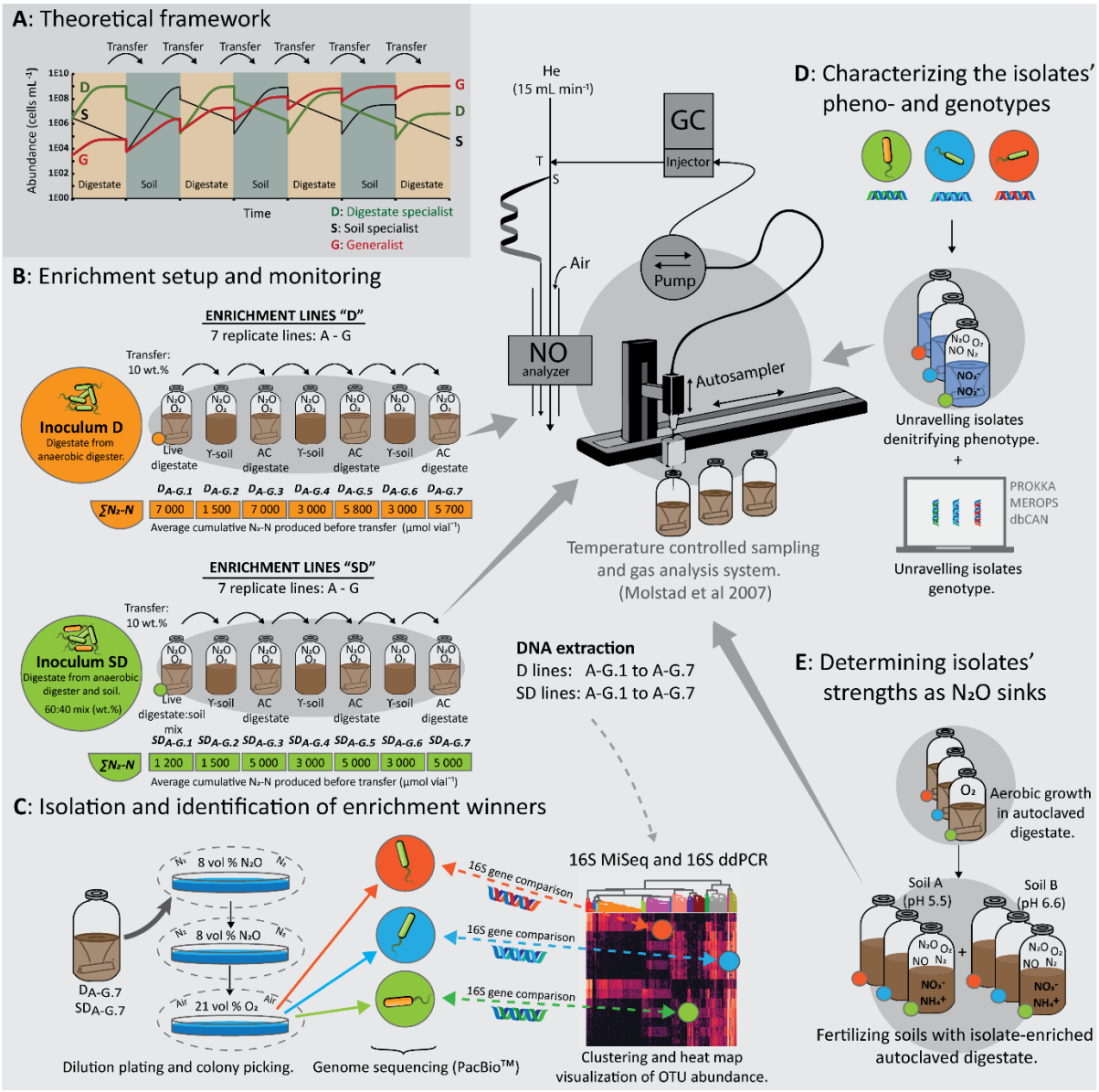


**Figure 1: Graphical summary of materials and methods**. **A:** The dual enrichment was modelled by a set of Lotka-Volterra logistic equations for three organisms; digestate specialist (D), soil specialist (S), and generalist (G), competing for a common substrate pool. The repeated transfer of enriched material from one enrichment to the next, alternating between soil and digestate, was predicted to enrich generalists by nature. The modelling is presented in detail in **Supplementary materials Section 1**: **Figs. S1** to **S6** and **Tab. S1**). **B**: Enrichment culturing experimental setup for the two enrichment lines "D" (digestate derived inoculum) and "SD" (soil and digestate derived mixed inoculum), each consisting of seven parallel replicate lines (A - G) over seven transfers. Each batch was supplemented with $O_2$ and $N_2O$ (He background) in the headspace and monitored for $O_2$, $N_2O$, and $N_2$ kinetics by frequent sampling of the headspace. While $O_2$ was allowed to deplete by respiration, $N_2O$ was sustained throughout by repeated injections. Average cumulative $N_2$ produced for each culture is indicated below vials (∑$N_2$-N). DNA was extracted from every vial at the conclusion of each enrichment. **C**: Extracted DNA was subjected to 16S rDNA amplicon sequencing, OTU clustering, and taxonomic assignment. The abundance of organisms circumscribed by each OTU was calculated from their relative abundance and the abundance of 16S rDNA $mL^{-1}$ as measured with digital droplet PCR (ddPCR). Relative abundance of the 500 most abundant OTUs throughout the enrichment was clustered using the Ward variance minimization algorithm. This allowed for identification of clades of OTUs with similar development throughout the dual enrichments. The OTUs 16S consensus sequences were aligned and matched with the 16S genes recovered from full genome sequencing of axenic $N_2O$-reducing isolates obtained from the final enrichments. **D**: The isolates' denitrifying phenotypes were assessed in pure culture incubations supplemented with either $NO_3^-$ or $NO_2^-$, and $O_2$ or $N_2O$ and $O_2$ and their phenotype matched against their denitrifying genotypes. Eco-physiological genome analysis by annotation of carbohydrate-active enzymes, peptidases, denitrification reductase genes, and other genes provided insight into the

suitability of these isolates as $N_2O$-reducing inoculants for soil inoculation. **E**: Each isolate was grown aerobically to high cell densities in autoclaved aerated digestate before amendment in two live soils (Soil A: pH 5.5 and Soil B: pH 6.6) supplemented $O_2$ and $NO_3^-$ to assess performance as $N_2O$-reducing inoculants in soil.

**Incubation- and gas measurement**

All incubations were done in 120 mL serum vials sealed with butyl-rubber septa, using a robotized incubation system (Molstad et al 2007, 2016) which monitors gas kinetics ($O_2$, $N_2$, $N_2O$, NO, $CO_2$ and $CH_4$) by repeated sampling of the headspace, returning an equal volume of He each time. Elaborated calculus routines, accounting for dilution by sampling and leakage (Bakken 2021) secures accurate estimates of production/consumption rates of each gas, electron flow rates to the various electron acceptors ($O_2$, $NO_3^-$, $NO_2^-$, NO, $N_2O$), and N mass-balance. Digestates and liquid cultures of isolated strains were stirred continuously (600 rpm) with a 23 mm Teflon-coated triangular magnet. Prior to incubation, the headspace air was replaced with He by repeated evacuation and filling with He and supplemented with pure $N_2O$ and/or $O_2$ (Molstad et al 2007).

**Digestate and soils**

The digestate was taken from the anaerobic digester of a municipal WWTP (Jonassen et al 2020), with chemical characteristics given in **Tab. S2**. Two clay loam soils were taken from a long-term liming experiment (Nadeem et al 2020), one with $pH_{CaCl2}$=6.6 (Soil A), and one with $pH_{CaCl2}$=5.5 (Soil B). Live digestate and live soil A were used in the initial enrichment cultures, while the substrates for subsequent enrichments (**Fig. 1B**) were autoclaved digestate (pH adjusted to 7.2 by titration with HCl), and ϒ-irradiated Soil A (25.9 kGy, 12 months prior to experiments). Digestate used for aerobic growth of the isolated $N_2O$-reducing bacteria before soil amendments (**Fig. 1E**) was autoclaved (121 °C, 20 min), then aerated by pumping sterile filtered air through a stirred suspension of digestate for 36 hours, and then pH adjusted to ~7.50-7.75 (**Tab. S2**) by titration with 4 M HCl. Aeration of the digestate was necessary in order to oxidize $Fe^{2+}$ in the digestate to $Fe^{3+}$, as otherwise the abiotic reduction of $O_2$ by $Fe^{2+}$ obscured measurements of oxygen consumption (Jonassen et al 2021).

**Dual enrichment culturing**

Enrichment series were started with two live materials: 50 mL digestate (**D-lines**) (pH 7.6±0.1) and 20 g Soil A + 30 mL digestate (**SD-lines**) (pH 7.2±0.1), each with 7 independent lines (A to G) (**Fig. 1A**). The nomenclature used throughout the text is: $D_{A\text{-}G,j}$ and $SD_{A\text{-}G,j}$, where D/SD denotes the initial live materials, *A-G* denotes the 7 independent replicates and *j* the enrichment number (1–7). $D_0$/$SD_0$ denotes live material before enrichment with $N_2O$. After replacing the headspace air with He, 3 mL $N_2O$, and 3 mL $O_2$ were injected into the vials, which were then incubated at 20 °C in the incubation system monitoring the $O_2$, $N_2O$ and $N_2$. Additional $N_2O$ was injected when needed to avoid $N_2O$ depletion. Subsequent enrichment cultures (j=2-7), alternating between γ-sterilized soil (45 g soil dry weight $vial^{-1}$+ 16 mL sterile water) autoclaved digestate (45 mL), were inoculated with ~10 wt% of the previous enrichment, following the same experimental procedure and conditions as explained above for the live starting materials. At the completion of each enrichment, samples were taken for DNA extraction and analysis and for isolation in the final enrichment.

**Community analysis**

DNA was extracted from technical duplicates, sampled at the conclusion of each enrichment cycle, from all $D_{A\text{-}G,j}$ and $SD_{A\text{-}G,j}$ vials (j = 1-7), the live materials ($D_0$ and $SD_0$), autoclaved digestate and ϒ-soil. DNA was extracted from 1 mL digestate slurry or 0.25 g soil using the PowerLyzer™ Soil DNA extraction kit (QIAGEN) following a modified kit protocol where bead beating for 30s at 4.5 $ms^{-1}$ in a MP Biomedicals™ FastPrep®-24 (Thermo Fischer Scientific Inc) replaced the vortexing step in the manufacturers protocol. Quantitative digital droplet PCR (ddPCR) was performed in technical triplicates on pooled samples of DNA extracts from biological and technical replicates from each enrichment cycle (j = 1-7), and pooled samples of technical replicate DNA extractions from $D_0$/$SD_0$, autoclaved digestate, and ϒ-soil, respectively. The ddPCR reaction mix (QX200 ddPCR EvaGreen® Supermix, BioRad) was prepared according to the manufacturer's instructions using the universal primers PRK341F (5'-CCTACGGGRBGCASCAG-3') and PRK806R (5'-GGACTACYVGGGTATCT-3') (Eurofins Genomic) targeting the V3-V4 region of the 16S rDNA gene (Yu et al 2005). The QX200 droplet generator (Bio-Rad) was used to generate oil droplet suspensions that were subjected to PCR with parameters given in **Tab. S3**. The PCR products were measured in a QX200 droplet reader (Bio-Rad), and the data analyzed in Quantasoft™ Analysis

Pro 1.0.596 software (Bio-Rad). Microbial community composition was determined through 16S rDNA amplicon sequencing (V3-V4 region) and taxonomic classification of 16S rRNA gene sequences. Library preparation and sequencing data processing were performed according to Nilsen et al (2020) except the library was quantified with the KAPA library quantification kit (universal; Roche) in a CFX96 Touch Real-Time PCR Detection System (Bio-Rad, USA). The amplicon library was diluted to 7 pM containing 20 % PhiX before sequencing on the MiSeq platform (Illumina, USA) using MiSeq reagent v3 kit to generate 300 bp paired-end reads. The sequencing produced 6139309 reads after quality filtering. The samples were rarefied at 9000 reads, resulting in the loss of 9 samples ($SD_{2.1}$-A, $SD_{7.6}$-B, $SD_{3.7}$-A, $SD_{7.7}$-A, $D_{1.1}$-A, $D_{1.3}$-B, $D_{2.3}$-A, $D_{2.4}$-A, $D_{3.6}$-A). The seaborn.clustermap in the Seaborn software suite (Waskom 2020) was used to generate hierarchically clustered heatmaps and was based on the Ward variance minimalization linkage algorithm (Ward 1963) for the 500 most abundant OTUs (sum abundance across all samples). Statistical analysis included principal component analysis (PCA) and similarity percentage (SIMPER) (Clarke 1996) using the PAST software (Hammer et al 2011). OTU absolute abundance was calculated as the product of its relative abundance and the abundance of 16S rDNA assessed by ddPCR for all OTUs (16S rDNA copies enrichment-vial$^{-1}$).

**Isolation and characterization of $N_2O$-reducing organisms**

Dilution series of the final enrichments ($D_{A-G,7}$ and $SD_{A-G,7}$) were spread on Sistrom's succinate medium (SS), R2-A, tryptic soy broth (TSB) and Nutrient broth (NB) agar plates (1.5 wt. %) (media composition is given in **Supplementary Materials Section 2**), incubated in $N_2$+ $N_2O$ atmosphere as described in Jonassen et al (2021) (**Fig. 1C**). Colonies were transferred to 120 mL vials containing 50 mL of the corresponding liquid medium and incubated aerobically with stirring (700 rpm) at 20 °C. 16S gene analysis showed that several different isolates were obtained, six of which were selected for full genome sequencing (working names in **bold**): *Aeromonas* sp. **AM**, *Ochrobactrum* sp. **OB**, *Pseudomonas* sp. **PS-02** and *Brachymonas* sp. (**BM**), which were isolated on SS medium, and *Cloacibacterium* sp. (**CB-01** and **03**) isolated on NB medium. Cultures were grown aerobically at 20 °C in SS (**AM, OB, BM, PS-02**) or NB (**CB-01**, **CB-03**) medium to $OD_{660} \approx 1.0$. After centrifugation, DNA was extracted from the pellets using PowerLyzer™ Soil DNA extraction kit (QIAGEN) as described above. The genomic DNA was sheared to approximately 8-14 kb long fragments and a library was generated with the SMRTbell Express Template Prep Kit 2.0 (PacBio) without size selection. The library was sequenced on a PacBio™ SMRT cell with the PacBio™ Sequel System using 3.0 chemistry at the Helmholtz Centre, Munich. After data demultiplexing, the genomes **CB-01**, **CB-03, BM,** and **AM** were assembled with the 'HGAP4' pipeline (SMRT Link Software, PacBio) with a seed coverage of 30 for **CB-01**, **CB-03,** and **BM**, and a seed coverage of 22 for **AM. PS-02** and **OB** were assembled with the 'Microbial Assembly' pipeline (SMRT Link Software, PacBio) with a seed coverage of 20 and 15, respectively. Genome quality was assessed with CheckM v1.0.18 (Parks et al 2015). Annotation of coding genes was done with Prokka v1.14.5 (Seemann et al 2014) using default parameters. The draft genomes were functionally annotated for carbohydrate-active enzymes (dbCAN2 meta server, Zhang et al 2018) and peptidases (MEROPS database, release 12.3) (Rawlings et al 2010). Signal P 5.0 (Raut et al 2021) was used to identify genes containing putative signal peptides as defined for gram negative bacteria. The denitrification regulatory phenotypes of the isolated strains was investigated by monitoring the kinetics of $O_2$, NO, $N_2O$, $NO_2^-$ and $NO_3^-$ in stirred batch cultures as they depleted the oxygen and switched to anaerobic respiration as described by Jonassen et al (2021). 200 µL samples of liquid culture were taken for $NH_4^+$ measurements and immediately stored at -20 °C before colorimetric analysis in LCK303 cuvettes (Hach Lange) in a DR 3900 spectrophotometer (Hach Lange).

**Evaluation of $N_2O$-reducing isolates as $N_2O$ sinks in soil**

The soils A and B were amended with five variations of digestate; **1:** live digestate (directly from the anaerobic digester), **2:** digestate heat treated to 70 °C for two hours, **3:** autoclaved pH-adjusted (7.75) digestate, **4:** autoclaved, aerated, and pH adjusted (7.75) digestate in which the isolates AM, BM, PS-02, CB-01 or OB had been grown by aerobic respiration, **5:** as 4, with CB-01, then heated to 70 $^0$C (2 h). Each variation was tested in duplicate 120 mL vials containing 10 g soil (Soil A or Soil B) (**Fig. 1E**) amended with 0.6 mL digestate (1-5) and 50 µmol $NO_3^-$ and 1 mL $O_2$ in a He atmosphere. Sterilized water was added to adjust the soil WFPS to 62 ± 1 % (Franzluebbers 1999). The vials were incubated at 20 $^o$C, and monitored for $O_2$, NO, $N_2O$ and $N_2$ (**Fig. 1D**). A follow-up experiment with the same experimental design was performed to test the dose dependence effect for

three of the isolates. Finally, we tested the persistence of the strains in soil, by making an identical extra set of vials (**1-5** above) which were stored aerobically in moist chambers, then amended with 1 mg $g^{-1}$ soil ground plant material (clover) to secure high metabolic activity, and incubated as described above.

To assess the effect of isolates on the potential $N_2O$ emission from denitrification in soil, we used the $N_2O$- index, $I_{N2O}$ (Liu et al 2014), which is the integral of the $N_2O$-curve divided by the integral of the total N-gas, for a given period (0-*T*):

$$I_{N_2O} = \frac{\int_0^T N_2O{-}N(t)dt}{\int_0^T [N_2O{-}N(t) + N_2{-}N(t) + NO(t)]dt} \quad (1)$$

The time period (*T*) is not fixed but set as the time when a given percentage of the available nitrogen oxyanions ($NO_3^-$+$NO_2^-$) are reduced to N-gas ($N_2$+$N_2O$+NO). In our case, we calculated $I_{N2O}$ for 40% and 100% recovery of nitrogen oxyanions as $N_2$+$N_2O$+NO (coined $I_{N2O40\%}$ and $I_{N2O100\%}$, respectively).

**Data availability**

The sequencing data for this study have been deposited in the European Nucleotide Archive (ENA) at EMBL-EBI under accession number PRJEB44171 (https://www.ebi.ac.uk/ena/browser/view/PRJEB44171).

## Results and discussion

### Dual enrichment culturing

To enrich and isolate $N_2O$-respiring organisms which can grow both in digestate and soil environments, we used a dual enrichment approach, i.e. sequential batch cultures, alternating between sterile digestate and sterile soil as substrates (**Fig. 1**). Each batch was provided with a small dose of $O_2$, to suppress obligate anaerobic organisms and select organisms capable of rapid transition from $O_2$- to $N_2O$-respiration. Subjecting the enrichments to recurrent changes (i.e. growth substrate, oxic/anoxic) selects for organisms with a capacity to adapt rapidly to changing environmental conditions (Brooks et al 2011), a desirable trait in an organism destined for soil amendment.

The kinetics of $N_2O$ reduction to $N_2$ throughout the consecutive enrichments is shown in **Fig. 2A** (more detailed analyses of the gas kinetics are shown in **Figs. S7** and **S8**). In the line D enrichment, which started from live digestate only ($D_{A\text{-}G.1}$), the $N_2$-kinetics indicated the presence of two populations of $N_2O$-respiring organisms; one whose activity was gradually declining, indicated by declining $N_2$-rates ($\mu$ = -0.03 $h^{-1}$), and a second population growing from initially extremely low numbers until their $N_2O$ respiration exceeded that of the declining population, increasing at a rate of 0.1 $h^{-1}$ (modelled in **Fig. S8**, top right panel). In contrast, theline SD enrichment, which started with a mixture of live soil and live digestate ($SD_{A\text{-}G\cdot1}$) showed exponentially increasing rates for $N_2$ production initially. Interestingly, the rates of $N_2$-production in $SD_{A\text{-}G\cdot1}$ did not reach as high as $D_{A\text{-}G.1}$ (~10 vs ~120 µmol $N_2$-N $h^{-1}$ $vial^{-1}$), which could be taken to suggest that a) the $N_2O$-reducing organisms originating from the soil quickly reached dominance due to the high initial numbers, b) these were less capable of scavenging electron donors in the digestate than the organisms originating from the digestate itself and/or c) the indigenous digestate bacteria were suppressed by the soil bacteria. Throughout the subsequent enrichments, the $N_2$-kinetics of the SD and D line became more similar, characterized by a short exponentially increasing rate, and subsequent more or less stable plateaus, probably reflecting an early depletion of the most easily available carbon substrates. The seven-replicate series within each line (D and SD) had remarkably similar kinetics, reflected in the marginal standard deviation (**Fig. 2A**).

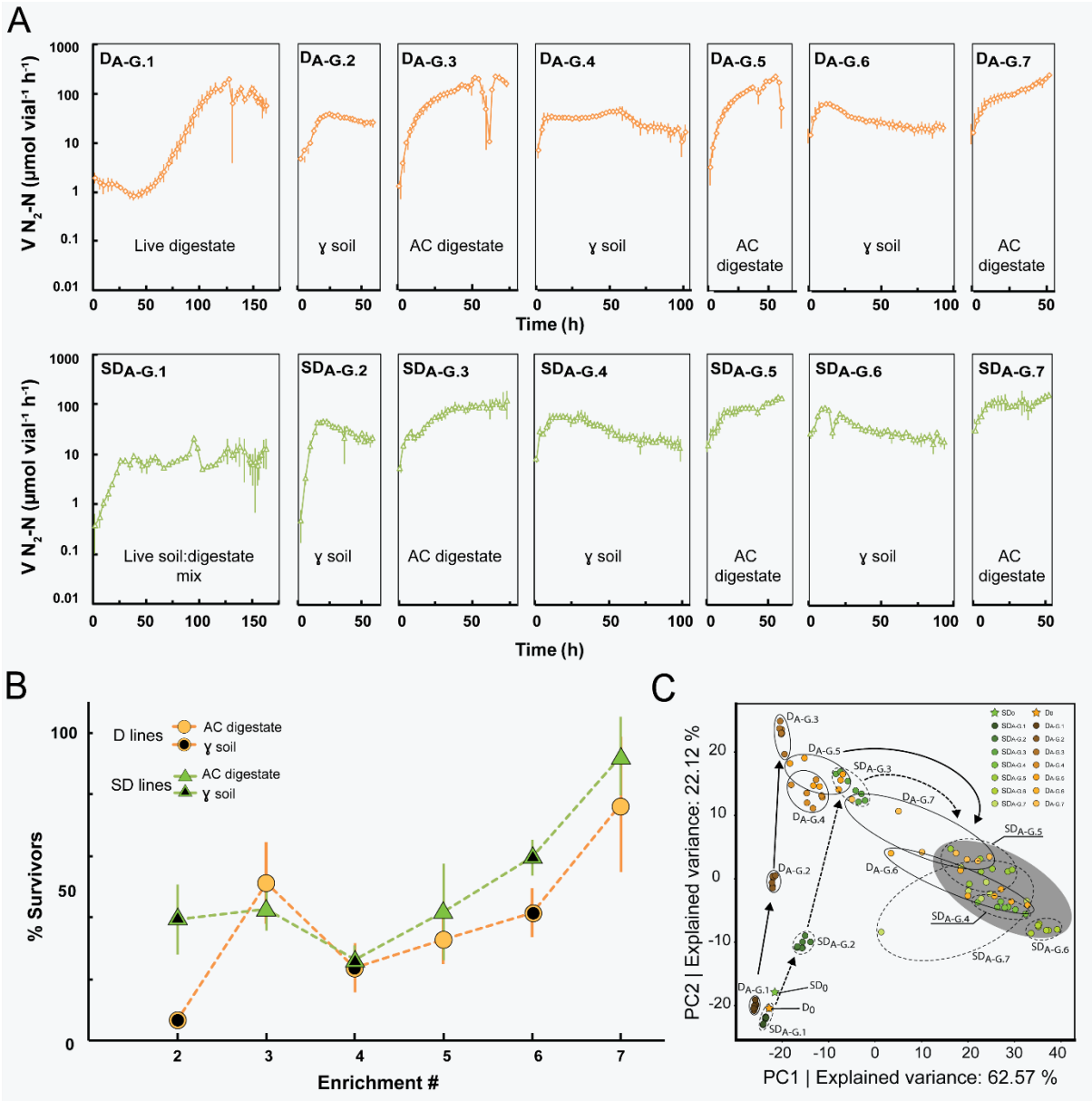


**Figure 2: Gas kinetics and PCA of enrichment cultures. Panel A:** Average rate of $N_2$-N production for the two lines of enrichment culturing. 10 weight % of enriched material was transferred from one replicate vial to the next ($D_{A\text{-}G.j}$ and $SD_{A\text{-}G.j}$ to $D_{A\text{-}G.j+1}$ and $SD_{A\text{-}G.j+1}$). AC digestate = autoclaved. ϒ soil = gamma sterilized. **Panel B**: Assessment of the fraction of the community surviving transfer to the next enrichment cycle (details in **Fig. S7). Panel C**: PCA of OTU relative abundances. Each dot represents an individual replicate (A-G). Standard deviation (n=7) is shown as vertical bars (panels A and B).

In theory (see supplementary **Figs. S1-S6**), the dual enrichment culturing should select for organisms that are able to grow both in soil and digestate (generalists **G**) over the organisms that can only grow in soil (soil specialists, **S**) and digestate (digestate specialists **D**), leading to a gradual increase in the G/(S+D) abundance ratio, which means that the percentage of $N_2O$-respiring cells that survive the transfer to a new substrate (from soil to digestate and *vice versa*) should increase. We achieved crude estimates of the % survivors for each transfer based on the cumulated $N_2$ in each enrichment and the initial rates in the next (explained in detail in **Fig. S9**), and the results (**Fig. 2B**) lend support to the hypothesis.

267 **Microbial community development in enrichment cultures**

268 The microbial community dynamics were analyzed based on 16S rRNA amplicon sequencing
269 and OTU clustering. PCA of community profiles demonstrated close similarity between
270 replicate vials (A-G) throughout the first three enrichments, and some divergence thereafter
271 (**Fig. 2C)**. SIMPER analysis revealed that 10 OTUs accounted for 94.4 and 93.5 % of the
272 explained variance in the D and SD line respectively, of which 8 OTUs were shared between
273 the two lines (**Tabs. S4** and **S5**). The D and SD lines followed similar trajectories and clustered
274 in proximity to each other from enrichment $SD_4$ and $D_6$ forward, indicating a convergence
275 towards a similar community structure (grey circle in **Fig 2C**). The PCA clearly verified that the
276 community underwent continuous dynamic succession and, surprisingly, that a high fraction
277 of dominant OTUs were shared between the two lines.

278 By targeted isolation of $N_2O$-respiring bacteria from the final enrichment cycle in autoclaved
279 digestate ($D_{A\text{-}G.7}$ and $SD_{A\text{-}G.7}$), we obtained seven axenic $N_2O$-respring cultures and sequenced
280 the genomes of six, using the PacBio sequencing platform (**Tab. S6**). The isolates were named
281 according to genera with which they clustered in the phylogenetic tree generated with the
282 16S rDNA gene sequences of the isolates and related strains (**Fig. S10**) and given working
283 names (**bold**): *Pseudomonas* sp. **PS-02**, *Aeromonas* sp. **AM**, *Brachymonas* sp. **BM**,
284 *Ochrobactrum* sp. **OB**, *Cloacibacterium* sp. **CB-01**, *Cloacibacterium* sp. **CB-03**, and *Azonexus*
285 sp. **AN**. **AN** was not genome sequenced, as its 16S partial sequence (obtained from Sanger
286 sequencing of 16S PCR amplicons using 27F/1492R primer pairs) matched the 16S gene (99.2
287 % sequence identity) of the dominating $N_2O$-reducing *Azonexus* sp. (ERR4842639) isolated
288 and characterized in the aforementioned experiments of Jonassen et al (2021).

289 The 16S genes recovered from the annotated genomes were compared to 16S of the OTUs
290 using usearch.global (Edgar 2010). This revealed high sequence identity (>97 %) in the
291 overlapping region (404 -429 bp) of the 16S rDNA consensus sequence of some OTUs, hence
292 these OTUs circumscribed the isolated species (**Tab. S7**). The isolates CB-01, CB-03, AN, BM
293 and PS-02 were circumscribed by OTU1, OTU1, OTU2, OTU8 and OTU19, respectively. These
294 OTUs represented four of the top six most abundant OTUs of the $D_{A\text{-}G.7}$ and $SD_{A\text{-}G.7}$ samples.
295 Including OTU74, circumscribing the isolate **OB**, five of the top 15 OTUs circumscribed the
296 isolates. Summed, the average abundances of these OTUs were 59.8 ± 1.2 % and 60.0 ± 1.1 %
297 in the $D_{A\text{-}G.7}$ and $SD_{A\text{-}G.7}$ enrichments, of which the dominating OTU1 accounted for 33 ± 10 %
298 and 39 ± 10 % of the total abundance.

299 The dynamic change in OTU abundance of the 500 most abundant OTUs (sum abundance
300 across all samples) throughout the consecutive enrichments of the D and SD lines was
301 hierarchically clustered based on Euclidian distance measures using the Ward´s linkage
302 algorithm (Ward 1963) and visualized by heatmapping of OTU abundance (**Fig. 3A)**. The
303 hierarchical clustering identified six clades, denoted A to E in **Fig. 3A**, that clustered OTUs
304 according to their abundance patterns throughout the consecutive enrichments. To achieve
305 a more quantitative assessment of the phenomena portrayed in the heatmap we combined
306 the total 16S rDNA gene abundance (**Tab. S8**) with the relative abundance of each clade and
307 individual OTUs (**Fig. 3BCD**). This analysis included an assessment of the relative increase of

individual OTUs from the consecutive enrichment cultures calculated as $R_i = \ln(N_{(i)}/(N_{(i-1)} \cdot 0.1))$, where $N_i$ is the estimated absolute abundance at the end of enrichment *i* and $N_{(i-1)}$ is the estimated absolute abundance at the end of the foregoing enrichment. The average $R_i$ for soil ($R_{soil}$) and for digestate-enrichments ($R_{Digestate}$) for each OTU was used to judge whether the OTU is a soil specialist (high $R_{Soil}$, low/negative $R_{Digestate}$), a generalist (high $R_{Soil}$ and $R_{Digestate}$) or a digestate specialist (high $R_{Digestate}$, low/negative $R_{Soil}$).

Most OTUs within Clade A were present initially in both enrichment lines ($D_0$ and $SD_0$), suggesting a primarily digestate origin of these OTUs, of which most were assigned to the phyla *Bacteriodetes*, *Cloacimonetes* and *Betaproteobacteria* (**Fig. 3A**). Clade A showed an increase in abundance throughout the enrichment in both enrichment lines (**Fig. 3B**) with an increase equivalent to ~5 cell divisions in the first 3-4 enrichment cultures (dashed line, **Fig. 3B**). Inspection of the growth of individual OTU's ($R_i$ values) within Clade A showed that they were able to grow both in digestate and soil, but they span a range from soil specialists ($R_{soil}$ close to zero) to generalists ($R_{soil}$ and $R_{digestate}$ >2, **Fig. S11**). The OTUs circumscribing the isolated cultures **CB-01** (OTU1), **CB-03** (OTU1), **AN** (OTU2), **PS-02** (OTU8), **AM** (OTU19) and **BM** (OTU37) were all within Clade A (**Fig. 3EF**). OTU2, circumscribing *Azonexus sp*. **AN**, grew better in digestate than in soil ($R_{Digestate}$ 3.40 ± 0.35 and $R_{Soil}$ 2.27 ± 0.35) and reached dominance in the first enrichment in live digestate ($D_{A\text{-}G.1}$ culture vials), which was also observed in the enrichments of Jonassen et al (2021).

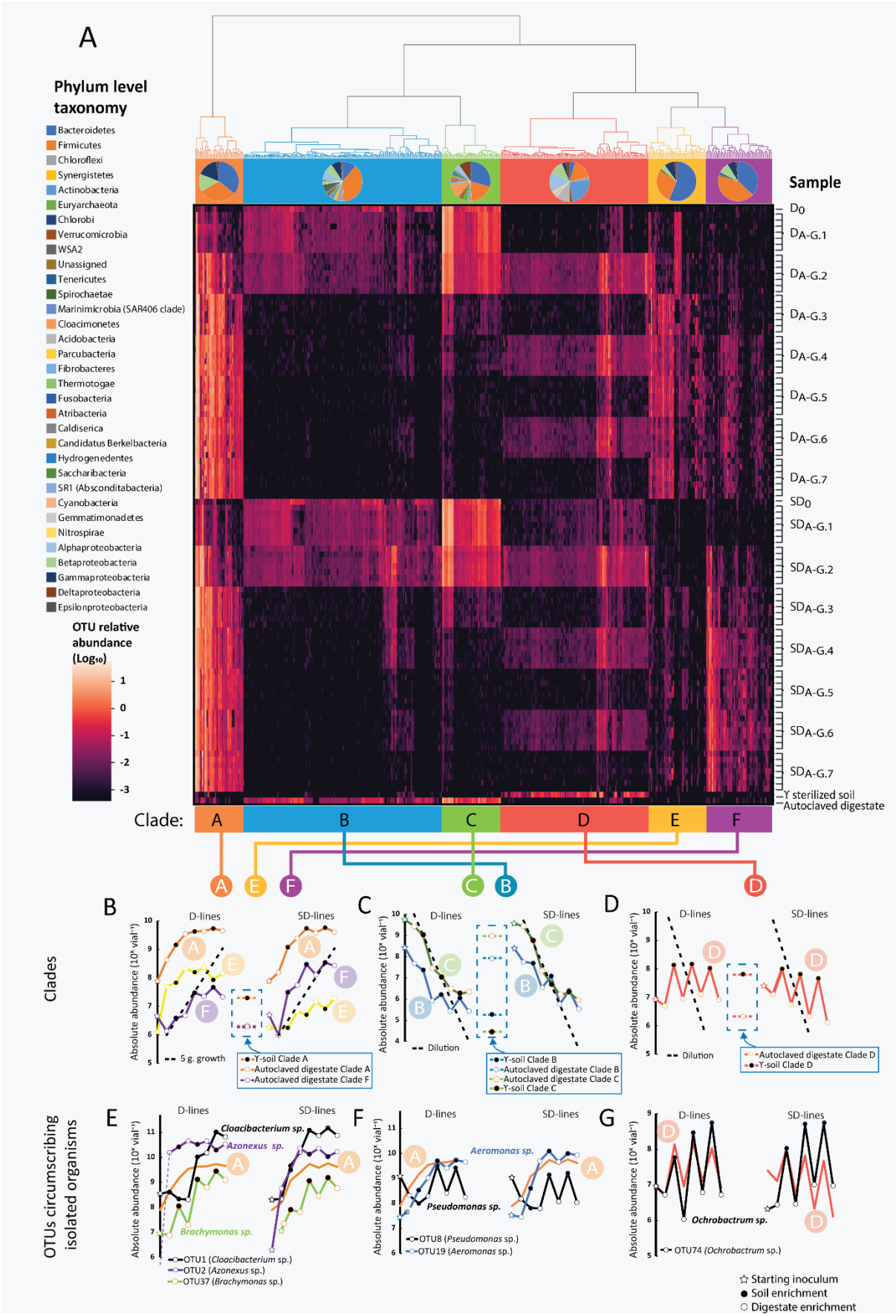


**Figure 3: Abundance of clustered OTU's throughout the dual enrichment culturing. Panel A:** Heatmapping and hierarchical clustering of the 500 most abundant OTUs from all biological replicates of the D line and SD lines of

the dual enrichment culturing, including starting inocula ($D_0$ and $SD_0$) and background samples of ϒ-soil and autoclaved digestate used as growth medium in the enrichments. OTUs are arranged in columns and samples in rows. The clustering has been delineated into six clades (A, B, C, D, E, F) with phylogenetic composition of OTUs in clades displayed below the cladogram. **Panels B-D** show the average absolute abundances (copies $vial^{-1}$=) for the OTU's within each clade throughout each enrichment; filled symbol= enrichment in soil, open symbol= enrichment in digestate, star = starting inoculum. The dashed lines in panels **C** and **D** represents the predicted decline by dilution, given a 10 % transfer rate, i.e. neither growth nor death. The dashed line in panel **B** represents a growth rate of 5 generations per enrichment. The OTU-abundancies in sterile materials are shown within dashed frames. **Panels E-G** shows the abundance of the OTU's which circumscribe the isolated strains, together with the averages of their resident clades.

Clade B and C plausibly harbored digestate derived OTUs, which were diluted out, rather than dying out, since their abundance declined with a rate largely as predicted by the dilution rate (**Fig. 3C** and **Figs. S12-13)**. In autoclaved digestate, the absolute abundance of OTUs clustered in clade B and C was ~$10^8$ and $10^9$ $vial^{-1}$ , respectively, while the abundance at the end of each enrichment was much lower, suggesting that their DNA is not destroyed by autoclaving, but that this relic DNA is degraded once the digestate is inoculated with live organisms. Thus, the high degree of clustering of samples by PCA (**Fig. 2C**) in the initial enrichments is probably not influenced by relic DNA as reported by others (Lennon et al 2018).

Clade D appeared to consist of soil specialist that sustained abundance in soil only, or alternatively, partly made up of relic DNA (DNA in the γ-sterilized soil) not metabolized during the enrichments in soil as mineral or humic substances may protect free DNA from rapid degradation (Nielsen et al 2007). However, some did appear to be true soil specialists due to their absence in the ϒ-sterilized soil (**Fig. 3A**). Our quantitative assessment confirmed that Clade D organisms grew in soil, while declining in digestate (**Fig. 3D**, and calculated *R* values **Fig. S14**). This clade harbored the soil specialist OTU74, circumscribing the isolated *Ochrobactrum* sp. **OB** (**Fig. 3G**), demonstrating the predicted characteristics of a soil specialist, reappearing at high abundance in soil enrichments.

Clade E showed an average increase in abundance throughout the enrichment in both enrichment lines but, interestingly, harbored organisms that were enriched to higher levels in the digestate derived line (D line) compared to the SD line (**Fig. 4B**), suggesting that they were suppressed by some organisms originating from the soil. Clade F appeared to contain organisms that were enriched in the SD line but remained at relatively low concentrations in the D line. OTUs of this clade were mostly soil derived organisms and their presence in the D line could be attributed to relic DNA (from the ϒ-soil) (Nielsen et al 2007) or an artifact of sequence OTU clustering.

**Eco-physiological genome analysis of isolated organisms.**

Throughout the enrichment series, the $N_2O$-respiring organisms were apparently growing under C-substrate limiting conditions most of the time (**Fig. 2A**), and tracing the OTUs circumscribing the isolated organisms throughout the enrichment cycles showed that many of these organisms grew to, and maintained, high abundance throughout the repeated transfers, i. e. growing in both materials (**Fig. 3EFG**). Acquisition of less accessible nutrients for growth and proliferation could therefore in part explain why the isolated organisms outperformed other species throughout the enrichments. To explore this metabolic

373 versatility, we annotated carbohydrate-active enzymes (CAZymes) and peptidases/proteases
374 in the isolate genomes using the dbCAN meta server (Zhang et al 2018) and the MEROPS
375 database (Rawlings et al 2010), respectively, and further analyzed the predicted proteins for
376 putative signal peptides using SignalP5.0 (Raut et al 2021).

377 A range of genes coding for CAZymes were identified in all isolates (**Tab. S9**), several of which
378 are known to target complex carbohydrates also contained putative signal peptides,
379 indicating that these proteins are transported to the cell exterior. Isolates **CB-01** and **CB-03**
380 seemed to have CAZymes focused on the breakdown of plant materials, coding enzymes
381 involved in degradation of cellulose, cellulose derivatives and starch (**Tabs. S9-10**). This was
382 supported by the presence of the carbohydrate binding module (CBM) 48, that binds to
383 various linear and cyclic α-glucans derived from starch and glycogen (Koay et al 2010, Chaen
384 et al 2012). **AM** had a large repertoire of genes encoding CAZymes with multiple CMBs
385 associated with binding to cellulose (CBM5, Kezuka et al 2006), starch/glycogen (CBM48),
386 peptidoglycans and chitin (CBM50, Onaga and Taira 2008) (**Tabs. S9-10**). All isolates, except
387 **BM,** had genes encoding cellulases, and genes encoding glycogen synthase (EC: 2.4.1.21 and
388 2.4.1.11) were recovered in **PS-02**, **AM**, **CB-01**, **CB-03** and **OB**. **AM** and **CB-01/CB-03** had
389 genes encoding glycogen operon protein glgX homolog (EC: 3.2.1.-) and glycogen
390 phosphorylase (EC: 2.4.1.1), both catalyzing breakdown of glycogen. This may be associated
391 with a fitness advantage during the dual culture enrichment as glycogen metabolism has been
392 shown to improve *E. coli* fitness when experiencing changing environments (Sekar et al 2020).
393 Contrastingly to the other isolates, **BM** did not appear to be geared towards extracellular
394 degradation of complex carbohydrates, nor contained genes involved in glycogen metabolism
395 (**Tabs. S9-10**) and might be dependent on harvesting easily available carbohydrates in the
396 sterilized growth media. Interestingly, the ability of the isolated strains to grow in sterilized
397 digestate was strongly related to the number of genes coding for proteases and CAZymes (**Fig.**
398 **S32H**)

399 All isolates encoded peptidases containing putative signal sequences, but the relative
400 proportion of these varied between the isolates; with **CB-03** having the largest proportion of
401 predicted peptidases containing putative signal sequences, followed by **AM** and **CB-01** (**Tab.**
402 **S11**). Extracellular secreted peptidases may also reflect environmental adaptations; the
403 isolates contained peptidases active at a more neutral pH range and known low-pH active
404 peptidases (Nguyen et al 2019) were not recovered. This falls in line with the inherent pH of
405 the environments from which the isolates were obtained – neutral/alkaline digestate and
406 weak acidic soil. Interestingly, the genomes **CB-01** and **CB-03** had several characteristics
407 similar to predatory bacteria, such as overrepresentation of genes for peptidases, genes for
408 the complete mevalonate pathway for isoprenoid production, histidine kinase (EC: 2.7.13.3),
409 serine protease (EC: 3.4.21.107), FMN NADH reductase (EC: 1.7.1.17, only recovered in CB-
410 01) and Dipate enol-lactone hydrolase (EC: 3.1.1.24) (Pasternak et al 2013). In contrast, **AB**,
411 **BM**, **OB** and **PS-02** encoded the complete MEP/DOXP pathway, common for non-predatory
412 bacteria (Pasternak et al 2013). We speculate that these genomic features may have
413 contributed to **CB-01** and **CB-03** achieving dominance throughout the enrichment, but, to the
414 best of our knowledge predatory traits of *Cloacibacterium* sp. has not been reported, and
415 further experimentation would be required to confirm this.

416 Species within the genus *Ochrobactrum* can fix nitrogen symbiotically in root-nodules (Trujillo
417 et al 2005, Zurdo-Pineiro et al 2007, Imran et al 2014).Some genes coding for proteins
418 involved nodule formation where recovered in *Ochrobacter* sp. **OB** genome (**Tab. S12**), but
419 not for the catalytic subunits of nitrogenase.

420 **Characterizing the isolates denitrifying regulatory phenotypes (DRP) and genotype**

421 All isolates did encode the gene for Nos, *nosZ* (clade I or II, Hein and Simon 2019), as well as
422 several other denitrification genes (**Fig. 4**). Although organisms with a full-fledged
423 denitrification pathway can both produce and reduce $N_2O$, they may be strong sinks for $N_2O$
424 in the environment, depending on their denitrification regulatory phenotype (**DRP**, Bergaust
425 et al 2011), which is shaped by the regulatory network controlling their stepwise reactions of
426 denitrification, both at the transcriptional (Spiro 2012) and metabolic (Mania et al 2020) level.

427 To characterize the DRP of our isolated strains, they were raised under strictly oxic conditions
428 to secure absence of any denitrification proteins, and transferred to gas-tight vials with liquid
429 medium containing 2 mM $NO_3^-$, and with He, $O_2$ and $N_2O$ in the headspace. As these stirred
430 cultures were allowed to deplete the oxygen and switch to anaerobic respiration, they were
431 monitored for $O_2$, NO, $N_2O$ and $N_2$ in the headspace and $NO_3^-$, $NO_2^-$ and $NH_4^+$ in the liquid.
432 Measured gases in incubations supplemented with 1 ml $O_2$, 1 mL $N_2O$ and 2 mM $NO_3^-$,
433 alongside with measured liquid concentrations of $NO_2^-$ $NO_3^-$ and $NH_4^+$ and genes coding for
434 catalytic subunits, are shown for each isolate in **Fig. 4**.

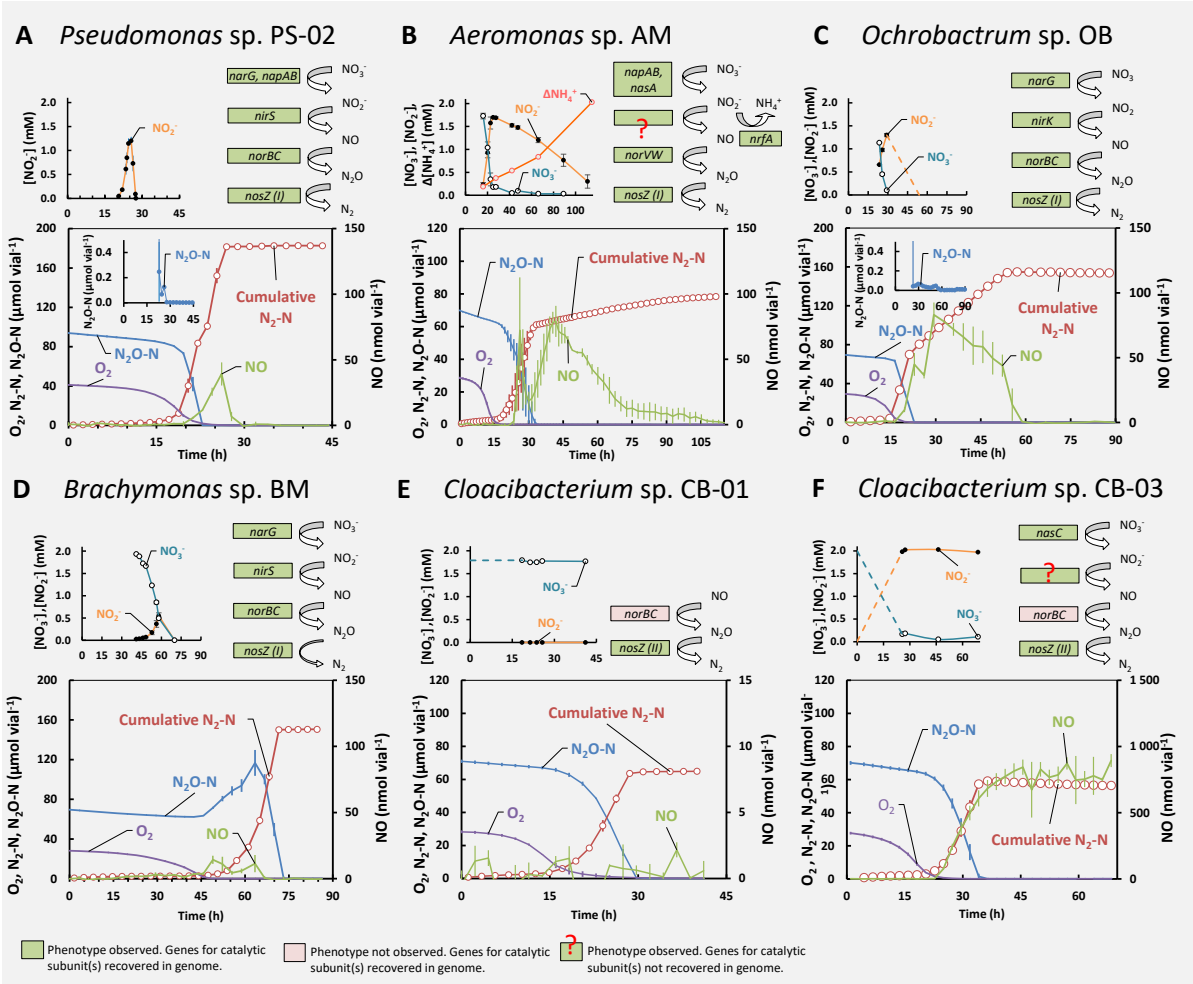


**Figure 4: Denitrification genes and denitrification phenotypes of isolated organisms.** Gas kinetics of $O_2$, $N_2O$-N, NO, and cumulative $N_2$-N (adjusted for leakage and sampling) in denitrifying phenotype experiments in 120 mL closed vials with He atmosphere containing 50 mL liquid growth medium supplemented with 1 mL $O_2$, 1 mL $N_2O$ and 2 mM $NO_3^-$. Liquid concentrations of $NO_2^-$, $NO_3^-$ and/or $NH_4^+$ (small panels, dashed lines = estimated by N-mass balance) and all genes coding for catalytic subunits of N-reductases recovered from the Prokka annotated genomes. **Panel A**: *Pseudomonas* sp. PS-01 (n = 2) grown in SS medium. PS-02 demonstrated strict control of gaseous denitrification intermediates throughout the incubation. **Panel B**: *Aeromonas sp.* AM (n = 3) grown in SS medium. AM demonstrated a DNRA+NOS phenotype, converting $NO_3^-$ to $NO_2^-$ and $NH_4^+$. Denitrification was ongoing throughout, but at a low and constant rate (0.4 µmol $N_2$-N $h^{-1}$ $vial^{-1}$, **Fig. S22**). **Panel C**: *Ochrobactrum* sp. OB (n = 2) grown in SS medium. OB demonstrated strict control of gaseous intermediates throughout the incubation. **Panel D**: *Brachymonas sp*. BM (n = 2) grown in Sistrom's succinate medium. BM demonstrated a full-fledged denitrifying phenotype where $N_2O$ was kept at high levels throughout the incubation. **Panel E**: *Cloacibacterium* sp. CB-01 (n = 3) grown in NB medium. CB-01 had a truncated denitrifying phenotype respiring primarily $N_2O$. **Panel F**: *Cloacibacterium* sp. CB-03 (n = 2) grown in NB medium. CB-03 had a truncated denitrifying phenotype converting $N_2O$ to $N_2$, and nitrate to nitrite.

The genomes of *Pseudomonas* sp. **PS-02**, *Ochrobactrum* sp. **OB** and *Brachymonas* sp. **BM**, predicted a full-fledged dentification pathway, i.e. reduction of $NO_3^-$ to dinitrogen gas, which was verified (**Fig. 4ACD**). However, theregulatory phenotypes were profoundly different: **PS-02** reduced available $NO_3^-$ and $N_2O$ concomitantly, before initiating $NO_2^-$-reduction (**Fig. 4A**). Nos activity was higher relative to the other N-reductases at the oxic/anoxic transition as there was only miniscule, transient accumulation of $N_2O$ during denitrification

458 ($NO_2 \rightarrow NO \rightarrow N_2O \rightarrow N_2$), and the preferential reduction of $N_2O$ was maintained if cultured with
459 $NO_2^-$, with or without $N_2O$ in the headspace (**Figs. S17** – **S20**). The phenotype of **OB** (**Fig. 4C**)
460 was very similar to that of **PS-02** and was maintained under a variety of conditions (**Figs. S21**
461 – **S24**). **BM**, however, reduced most of the available $NO_3^-$ to $N_2O$ at first (**Fig 4D**), and this trait
462 was retained if cultured with $NO_2^-$, with or without $N_2O$ in the headspace (**Figs. S25** – **S27**).
463 This suggested that while **BM** would be a source of $N_2O$ in the environment, **PS-02** and **OB**
464 would be strong sinks.

465 DNRA organisms with *nosZ* could be attractive inoculants since they reduce $NO_3^-$ to $NH_4^+$
466 rather than to $N_2$, thus retaining plant-available N in the soil (Rütting et al 2011), and at the
467 same time scavenging $N_2O$ produced by other organisms. The AM isolate simultaneously
468 reduced the available $NO_3^-$ to $NO_2^-$ and $N_2O$ to $N_2$ after $O_2$-depletion (**Fig. 4B,** analyzed in more
469 detail in **Fig. S28**), and subsequently reduced $NO_2^-$ to $NH_4^+$ and trace amounts of $N_2$. This
470 indicated dissimilatory nitrate reduction to ammonium (DNRA), which was corroborated by
471 the presence of *nrfA* in the genome, coding for a key enzyme of DNRA (Cytochrome c552
472 nitrite reductase, EC: 1.7.2.2) (Einsle, 2011). It also carried a *nasD* gene that showed high
473 sequence similarity (protein blast) with NirB (NADH-dependent nitrite reductase) of a related
474 *Aeromonas media* strain. Genes for the nitrite reductases NirS/K were not identified, and the
475 source for the produced NO remains unresolved. The **AM** genome also apparently lacked
476 genes for the nitrate reductase NarGHI, while genes coding for periplasmic nitrate reductase
477 Nap (*napAB*) and $N_2O$ reductase Nos (*nosZ*, clade I) were present. It also encoded the gene
478 *nasA*, which showed high sequence similarity (protein blast) to a nitrate reductase of a related
479 *Aeromonas media* strain. NasA is a constituent of the nitrate assimilatory system (Nas) and
480 functions as a nitrate reductase in nitrate assimilation in a wide range of bacteria (Jiang et al
481 2015). The phenotypic analysis (**Fig. 4B**) showed that $NO_3^-$ and $N_2O$ were clearly reduced at
482 the same time in incubations with the **AM** isolate. This contrasts earlier findings that Nos
483 outcompetes Nap (for electrons) in denitrifying bacteria (Mania et al 2020), and it could be
484 speculated that the gene annotated as NasA in **AM** may be responsible for the reduction of
485 $NO_3^-$ to $NO_2^-$ that took place concomitantly with $N_2O$ reduction. However, none of the other
486 genes generally found in the *nas* operon of bacteria, such as *nasFEC* and *B*, were detected in
487 the genome analysis.

488 The genotypes of *Cloacibacterium* sp. **CB-01** and **CB-03** predicted a truncated denitrification
489 pathway ($NO \rightarrow N_2O \rightarrow N_2$), and one (CB-03) was also equipped with genes for assimilatory $NO_3^-$
490 reductase (*NasC*, EC: 1.7.99.4) and a nitrite/nitrate transporter (*narK*). This was all verified by
491 experiments showing stoichiometric conversion of $N_2O$ to $N_2$ and reduction of $NO_3^-$ to $NO_2^-$
492 by **CB-03** (**Fig. 4EF**) and corroborated by experiments under a variety of conditions (**Figs. S29-**
493 **S31**). The early onset of $NO_3^-$ reduction, before depletion of oxygen, suggesting that NasC was
494 active under oxic conditions in this isolate, which was also reported for *Paracoccus*
495 *denitrificans* (Pinchbeck et al 2019). Of the two isolates, **CB-01** makes for a particularly
496 promising $N_2O$-reducing soil inoculant. Both **CB-01** and **CB-03** were circumscribed by the
497 dominating OTU1 of Clade A (**Fig. 3E**) which dominated in both D and SD enrichment lines.

498 **Performance of isolated organisms as sinks for $N_2O$ in soil**

To produce inocula for testing isolates' capacity as $N_2O$ sinks in soil, they were grown aerobically to high cell densities in autoclaved digestate (**Fig. S32**). The estimated the cell density at the end of the 45 h incubation was ranged from 0.5 to 1.4 mg dry-weight $mL^{-1}$ ( ~3-7 · $10^{10}$ cells $mL^{-1}$) for the different isolates, the lowest value recorded for *Brachymonas* sp. **BM** (0.5) while Aeromonas sp. **AM** reached highest (1.4). Interestingly, the capacity of the isolates to grow was strongly correlated with the number of genes coding for CAZymes and proteases in their genomes (**Fig. S32H**).

To assess the $N_2O$ sink capacity of these aerobically grown organisms, they were inoculated to soil in vials with He atmosphere (with traces of $O_2$), which were monitored for $O_2$, NO, $N_2O$ and $N_2$. Since the effect of such inoculation confounds the effect of the isolates and the effect of the available carbon in the autoclaved digestate, we included a set of control treatments. Thus, the experiment included 5 different pre-amendments: 1) Autoclaved digestate enriched with isolate by aerobic growth, 2) live digestate sampled directly from the anaerobic digester, 3) live digestate heat-treated to 70 °C for two hours (70 °C digestate) to reduce the activity of native $N_2O$ producers (Jonassen et al 2021) 4) digestate in which CB-01 was grown, subsequently heated to 70 °C for two hours (70 °C $O_2$ dig) to give comparable amounts of carbon added to the soil, and 5) soil without any amendments. The $I_{N2O}$-emissions ratio, which is the area under the $N_2O$-curve divided by the area under the $N_2O$+$N_2$-curve (Liu et al 2014; Russenes et al 2016) expressed as a percentage, was used as a proxy to assess the treatment effects in the amended soils (**Fig. 5**).

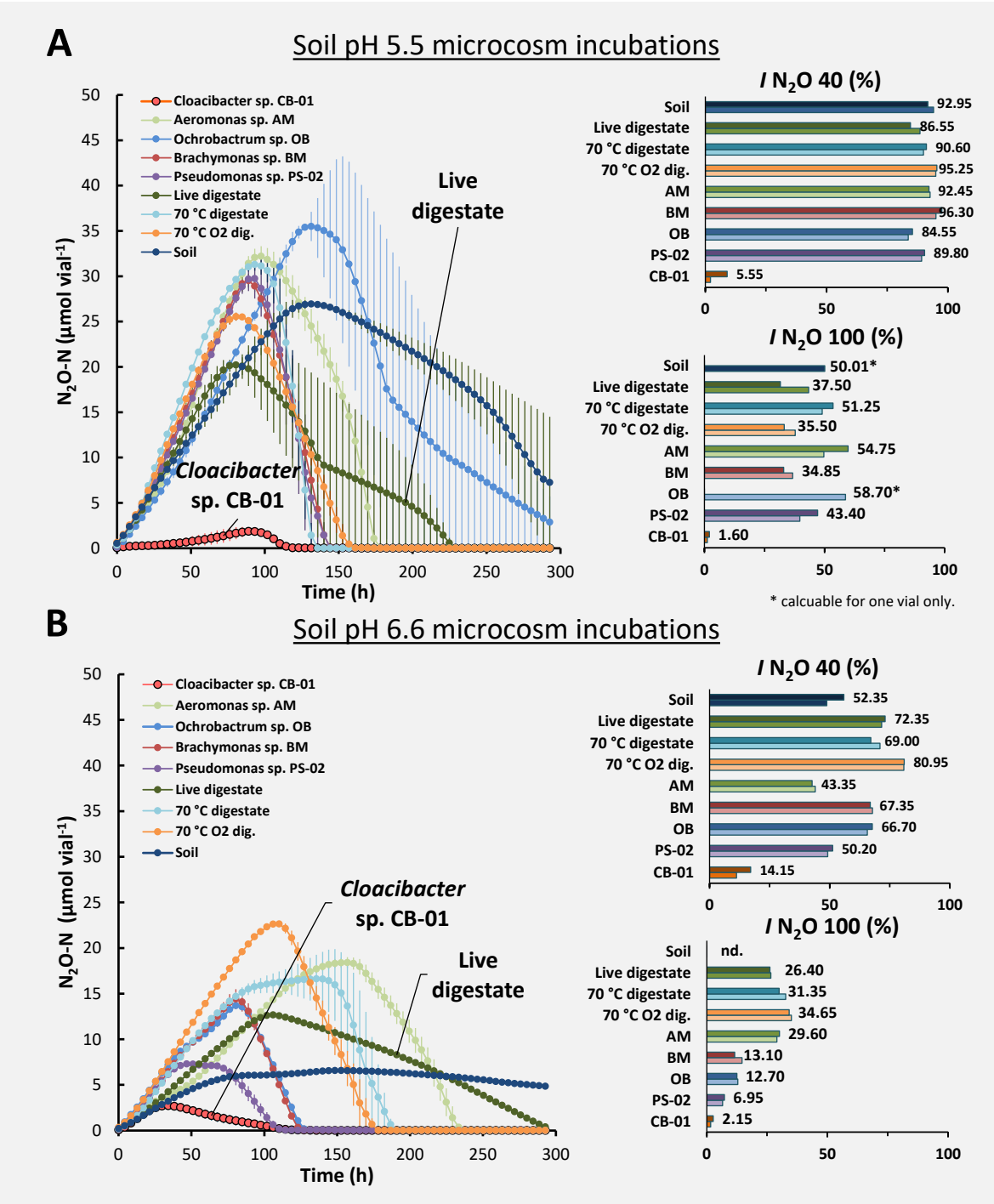


**Figure 5:** Gas kinetics during incubation of soils (**Panel A**: soil pH=5.5, **Panel B**: soil pH=6.6) amended with various pretreated digestates (0.06 mL $g^{-1}$ soil): "Live digestate" = digestate directly from the anaerobic digester, "70 °C digestate" = live digestate heat treated to 70 °C for two hours, "70 °C $O_2$ dig." = autoclaved digestate used to grow strain CB aerobically, and then heat treated to 70 °C for two hours. **AM**, **BM**, **OB**, **PS-02** and **CB-01**: autoclaved digestate in which strains **AM, BM, OB, PS-02 and CB-01** had been grown aerobically.) to cell densities of 1.39, 0.51, 0.79, 0.81 and 0.72 mg cell dry-weight $mL^{-1}$, respectively (**Fig. S32**). The main graphs (panels A&B) show $N_2O$ kinetics for each treatment (n = 2). The two bar graphs to the right show the $N_2O$ indexes (***$I_{N2O}$***, single vial values), which is the area under the $N_2O$-curve divided by the area under the $N_2O$+$N_2$-curve expressed as a percentage. Two ***$I_{N2O}$*** values are shown: one for the timespan until 40% of the $NO_3^-$-N is recovered as $N_2$+$N_2O$+NO-N (**$I_{N2O\ 40\%}$**), and one for 100% recovery (**$I_{N2O\ 100\%}$**). More details (including $N_2$ and NO kinetics) are shown in **Figs. S33 and S34.**

531 As expected, $I_{N2O}$ values were generally higher in the pH 5.5 soil than in the pH 6.6 soil (**Fig.**
532 **5B**), and the isolates BM, OB, PS-02 lowered $I_{N2O}$ only in the soils with pH 6.6. CB-01, however,
533 resulted in extremely low $I_{N2O}$ values in both soils, clearly outperforming any of the control
534 treatments. We tested if the ability of **CB-01** to act as a strong $N_2O$ sink in the pH 5.5 soil could
535 be due to acid tolerance, by growing the organisms in stirred (600 rpm) liquid medium with
536 pH ranging from 5.5 to 7, and found no evidence for acid tolerance, neither for growth nor
537 for the synthesis of functional $N_2O$-reductase (**Fig. S31)**. An alternative explanation of the
538 acid-tolerant $N_2O$-sink effect of **CB-01** could be that the cells were embedded in
539 flocks/biofilms in the digestate, protected against low soil-pH by the buffer- capacity of the
540 matrix. Strains of *Cloacibacterium* are known to secrete extracellular polymeric substances
541 (Nohua et al 2015) and found in high abundance in biofilms of natural (Pang et al 2016), which
542 lends support towards the hypothesis of matrix mediated shielding effects. This points
543 towards the advantages of biofilm formation or other attachment strategies in generating
544 favorable micro niches and so gaining advantage over competitors in a low pH environment.

545 Whilst our eco-physiological genome analysis revealed that several isolates had the genetic
546 potential to utilize complex carbon sources and encoded several traits that might secure
547 survival in a competitive situation, agricultural inoculants are most definitely invaders of the
548 soil microbial community, and any longer-term establishment is dependent on the resistance
549 by the residential community against alien species. The likelihood of a successful invasion is
550 related to the resident community richness, referred to as the diversity-invasion effect
551 (Mallon et al 2018), and reflects the key challenges of an invading organism; growth and
552 establishment by utilizing resources not utilized by the resident community, or forcefully
553 "overtake" a resident niche through competition or antagonism.

554 To assess the ability of our isolates to persist in soil and to retain their $N_2O$ reduction capacity,
555 a second experiment was set up with identical treatments to those in **Fig. 5**, but storing the
556 amended soils for 1 month before testing the denitrification kinetics. A fertilization event was
557 simulated by the addition of 50 µmol $NO_3^-$, 1 mg ground plant material $g^{-1}$ soil, and 0.5 mL $O_2$
558 before sealing vials and monitoring denitrification kinetics throughout depletion of oxygen
559 and the transition to anoxia. In this experiment the effect of the inoculated isolates on $N_2O$ -
560 emissions was evaluated based on maximum $N_2O$ accumulation (no treatment reduced all
561 available N-oxides, making it impossible to calculate $I_{N2O}$ emission indexes) (**Figs. S35-36**).
562 Whilst none of the inoculants significantly differed from the controls in pH 5.5 soil, PS-02
563 outperformed the other inoculants at pH 6.6. In fact, the soil treated with **PS-02** performed
564 better after 30 days soil storage (maximum $N_2O$ for PS-02 was ~1/10 of other treatments, **Fig.**
565 **S36**) than immediately after amendment in the first soil experiment (**Fig. 5**). Likewise,
566 maximum $N_2O$ for **CB-01** treatment in pH 6.6 soil was approximately 2/3 of other
567 amendments, but the difference was not statistically significant ($p > 0.05$).

568 A dose-response experiment with the isolates **CB-01**, **PS-02**, and **OB** was conducted to
569 determine the minimum dose needed to obtain substantial reduction of $N_2O$ production in
570 soil. The isolates were grown aerobically in autoclaved digestate (pH adjusted to 7.5) as
571 explained above, the cell density achieved was assessed by the cumulated oxygen
572 consumption (explained in detail in **Fig. S37**), and the cell density was adjusted to 0.3 mg cell

573 dry-weight $mL^{-1}$ for all three strains, by dilution with autoclaved digestate. These enriched
574 digestates were then used in an amendment experiment identical to that presented in **Fig. 5**,
575 but with three different doses of enriched digestates (0.6, 0.3 or 0.15 mL; triplicates for each
576 level), which is equivalent to an inoculation intensity of 18, 9 and 4.5 µg cell dry-weight $g^{-1}$
577 soil, or 9, 4.5 and $2.3 \cdot 10^7$ cells $g^{-1}$ soil, assuming the same dry-weight per cell as *Paracoccus*
578 *denitrificans* ($2 \cdot 10^{-13}$ g dw $cell^{-1}$). The highest inoculation intensity in this experiment is
579 approximately 50% of that used in the previous experiments (**Fig. 5**). The experiment included
580 controls, amended with equivalent doses of sterile pre-aerated autoclaved digestate.

581 The results (summarized in **Fig. S38** and **Tab. S13)** showed a strong and dose-dependent
582 effect of *Cloacibacterium* sp. **CB-01** on the $N_2O$ accumulation, exemplified with the peak $N_2O$
583 concentration (Max $N_2O$), which was reduced by 96, 64 and 20% (compared to the control
584 without bacteria) by the inoculation levels 0.6, 0.3 and 0.15 mL digestate $vial^{-1}$, respectively
585 ($p<0.05$ for all contrasts). *Pseudomonas* sp. **PS-02** and *Ochrobacter* sp. **OB** had weaker effects
586 on Max $N_2O$, but statistically significant ($p<0.05$) at all inoculation levels. The $\boldsymbol{I_{N2O}}$ showed the
587 same patterns, but several contrasts (bacteria versus control) lacked statistical significance
588 for the lowest inoculation level.

589 Our inoculation levels were 2.7, 4.5 and $9 \cdot 10^7$ cells $g^{-1}$ soil, which is within the upper range of
590 inoculation levels used by Domeignoz-Horta et al (2016), who inoculated soils with $10^6$ and
591 $10^8$ *Dyadobacter fermentans* - cells $g^{-1}$ soil. *Dyadobacter fermentans* carry *nosZ* Clade II, but
592 no other denitrification genes, which makes it comparable to our *Cloacibacterium* sp. CB-01,
593 and a comparison of the performance of the two strains is interesting: inoculation with $10^8$ *D.*
594 *fermentans* – cells $g^{-1}$ resulted in a reduction in the $N_2O/(N_2O+N_2)$ product ratio which is
595 similar to what was achieved by the two highest inoculation levels with *Cloacibacterium*, i.e.
596 $0.45\text{-}0.9 \cdot 10^8$ cells $g^{-1}$. Thus, the two strains appear to have similar capacities for acting as sinks
597 for $N_2O$ in soil. However, a closer inspection of the data reveals that *Dyadobacter* did not
598 affect the $N_2O$-emission in soils with pH below 6.6, while *Cloacibacterium* performed well in
599 our acid soil (pH 5.5, **Fig 5A**). This could indicate that *Cloacibacterium* sp. **CB-01** has a more
600 robust $N_2O$ sink capacity in low-pH soils. As suggested previously, this is probably not due to
601 an inherent acid tolerance, but rather a combined effect of the organisms' tendency to
602 aggregate and form biofilms, and the relatively high pH of the digestate (7.6). The matrix in
603 which cells are embedded prior to inoculation to soils is probably a crucial issue.

604 **Concluding remarks**

605 The hierarchical clustering of 16S rRNA-based OTUs demonstrated that the dual enrichment
606 effectively selected "generalist organisms" capable of growth by $N_2O$-respiration both
607 sterilized digestate and soil, already after 3-4 transitions, as predicted by the model. (**Figs. S1**
608 to **S5**).

609 Among the isolates, *Cloacibacterium* sp. **CB-01** stand out as particularly interesting because it
610 grew well both in soil and digestates and was unable to denitrify *sensus stricto* (lacking the
611 genes for dissimilatory $NO_3^-$ and $NO_2^-$ reduction). In addition, it proved a strong $N_2O$ sink even
612 in the acid soil (pH 5.5), where the other isolates appeared unable to synthesize functional
613 $N_2O$ reductase, as is the case for most organisms (Liu et al 2014, Lim et al 2021). Testing the

614 pH-response of CB-01 in pure culture showed no particular tolerance to low pH (**Fig. S30**). We
615 speculate that its ability to reduce $N_2O$ in low pH soil is due to the ability of this organism to
616 localize in alkaline microinches supplied by the digestate material, possibly through the
617 production of a biofilm, a trait known to be common to members of this genus (Tiirola et al
618 2009, Revetta et al 2013, Biswas et al 2014, Pang et al 2016). The ability to retain activity in
619 low pH soils is very desirable for agriculture due to the issue of soil acidification, driven by N-
620 input and subsequent base cation depletion in agricultural soils (Tian et al 2015), and the
621 uncertainty in net GHG-emission reduction of the few viable treatment options such as liming
622 (Wang et al 2018, Hénault et al 2019) to mitigate $N_2O$ derived from denitrification in these
623 soils, but at a possible expense of increased emissions of carbonate-$CO_2$ (Wang et al 2021).
624 The second isolate to show promise is **PS-02**. While **PS-02** can act as both a source and sink
625 for $N_2O$, it showed the benefit of eliciting an $N_2O$-emissions reduction for an extended period
626 after soil amendment. An interesting possibility and a future perspective is the option of
627 combining **PS-02** and **CB-01**, to secure effective elimination immediately after fertilization
628 (**CB-01**) as well as a more long-lasting effect (**PS-02**).

629 Not all the members of the generalist Clade A OTUs were obtained as pure cultures and
630 extended isolation efforts may uncover yet more organisms with good qualities for an
631 amended digestate material. Further, this enrichment technique could easily be expanded to
632 new soils and new digestates to develop amendments suited to specific local materials and
633 conditions. Future research investigating the performance of digestate amendments derived
634 from these isolates would be valuable to accurately quantify the $N_2O$-emissions reduction
635 effects under field conditions.

636 **Acknowledgements**

637 This work was financially supported by the Norwegian Research Council (project number:
638 260868). We wish to thank Elisabeth G. Hiis for indispensable assistance with the automated
639 gas incubation and measurement system.

## References:


Bakken LR (2021) Spreadsheet for gas kinetics in batch cultures. Researchgate DOI: 10.13140/RG.2.2.19802.36809

Bergaust L, Bakken L, Frostegård Å (2011) Denitrification regulatory phenotype, a new term for the characterization of denitrifying bacteria. Biochemical Society transactions. 39. 207-12. Doi: 10.1042/BST0390207.

Braman SR, Hendrix SA (1989) Nanogram nitrate and nitrite determination in environmental and biological materials by vanadium(III) reduction with chemiluminescense detection. Anal Chem 61: 2715-2718

Butterbach-Bahl K, Baggs EM, Dannenmann M, KieseR, Zechmeister-Boltenstern S (2013) Nitrous oxide emissions from soils: How well do we understand the processes and their controls? Philosophical Transactions of the Royal Society B: Biological Sciences, 368: 20130122.

Caporaso JG, Kuczynski J, Stombaugh J, Bittinger K, Bushman FD, Costello EK, Fierer N, Peña AG, Goodrich JK, Gordon JI, Huttley GA, Kelley ST, Knights D, Koenig JE, Ley RE, Lozupone CA, McDonald D, Muegge BD, Pirrung M, Reeder J, Sevinsky JR, Turnbaugh PJ, Walters WA, Widmann J, Yatsunenko T, Zaneveld J, and Knight R (2010) QIIME allows analysis of high-throughput community sequencing data, *Nature methods*, 7: 335-36.

Chaen K, Noguchi J, Omori T, Kakuta Y, Kimura M (2012) Crystal structure of the rice branching enzyme I (BEI) in complex with maltopentaose. Biochemical and biophysical research communications, 424(3), 508-511.

Cosentino S, Larsen MV, Aarestrup FM, Lund O (2013) PathogenFinder - distinguishing friend from foe using bacterial whole genome sequence data. Plos One 8. doi:10.1371/journal.pone.0077302

Cox RD (1980) Determination of nitrate and nitrite at the parts per billion level by chemiluminescence. Analytical Chemistry 52, 332–335. http://dx.doi.org/10.1021/ ac50052a028.

Davidson EA (2009) The contribution of manure and fertilizer nitrogen to atmospheric nitrous oxide since 1860. Nat. Geosci. **2**, 659–662

Domeignoz-Horta LA, Putz M, Spor A, Bru D, Breuil MC, Hallin S (2016) Non-denitrifying nitrous oxide reducing bacteria – an effective N2O sink in soil. Soil Biol Biochem 103:376-379.

Edgar RC (2010) Search and clustering orders of magnitude faster than BLAST, *Bioinformatics* 26(19), 2460-2461, doi: 10.1093/bioinformatics/btq461

Edgar RC (2013) UPARSE: highly accurate OTU sequences from microbial amplicon reads, *Nature methods*, 10: 996-8.

Einsle O (2011) Structure and function of formate-dependent cytochrome c nitrite reductase, NrfA. Methods in enzymology, 496, 399-422. https://doi.org/10.1016/B978-0-12-386489-5.00016-6

Forster P, Ramaswamy V, Artaxo P, Berntsen T, Betts R, Fahey DW, Haywood J., et al. Solomon S, Qin D, Manning M, Chen Z, Marquis M, Averyt KB, Tignor M, et al. (2007) Changes in atmospheric constituents and in radiative forcing, Climate Change 2007: the Physical Science Basis. Contribution of

Working Group I to the Fourth Assessment Report of the Intergovernmental Panel on Climate Change, Cambridge, Cambridge University Press (pg. 129-234).

Franzluebbers AJ (1999) Microbial activity in response to water-filled pore space of variably eroded southern Piedmont soils, Applied Soil Ecology, Volume 11, Issue 1, Pages 91-101, ISSN 0929-1393, https://doi.org/10.1016/S0929-1393(98)00128-0

Gardner AM, Gessner CR, Gardner PR (2003) Regulation of the nitric oxide reduction operon (norRVW) in Escherichia coli. Role of NorR and sigma54 in the nitric oxide stress response. The Journal of biological chemistry, 278(12), 10081–10086. https://doi.org/10.1074/jbc.M212462200

Graf DR, Jones CM, Hallin S (2014) Intergenomic comparisons highlight modularity of the denitrification pathway and underpin the importance of community structure for N 2 O emissions. PloS one, 9(12), e114118.

Hammer Ø, Harper DAT, Ryan PD (2001) PAST: Paleontological statistics software package for education and data analysis. *Palaeontologia electronica* 4.1: 9.

Hein S, Simon J (2019) Bacterial nitrous oxide respiration: electron transport chains and copper transfer reactions. *Advances in microbial physiology*, *75*, 137-175.

Hénault C, Bourennane H, Ayzac A et al (2019) Management of soil pH promotes nitrous oxide reduction and thus mitigates soil emissions of this greenhouse gas. Sci Rep **9,** 20182. https://doi.org/10.1038/s41598-019-56694-3

Imran A, Saadalla MJA, Khan SU, Mirza MS, Malik KA, Hafeez FY (2014) Ochrobactrum sp. Pv2Z2 exhibits multiple traits of plant growth promotion, biodegradation and N-acyl-homoserine-lactone quorum sensing. Annals of Microbiology, 64(4), 1797-1806.

Jiang X, Dang H, Jiao N (2015) Ubiquity and Diversity of Heterotrophic Bacterial nasA Genes in Diverse Marine Environments. PLoS ONE 10(2): e0117473. doi:10.1371/journal.pone.0117473

Jonassen KR, Hagen LH, Vick SHW, Arntzen MØ, Eijsink VGH, Frostegård Å, Lycus P, Molstad L, Phillip B. Pope PB, Bakken LR (2020) Bacteria in digestates for reduced climate forcing, bioRxiv.

Kezuka Y, Ohishi M, Itoh Y, Watanabe J, Mitsutomi M, Watanabe T, Nonaka T (2006) Structural studies of a two-domain chitinase from Streptomyces griseus HUT6037. Journal of molecular biology, 358(2), 472-484.

Koay A, Woodcroft B, Petrie EJ, Yue H, Emanuelle S, Bieri M, Bailey MF, Hargreaves M, Park JT, Park KH, Ralph S, Neumann D, Stapleton D, Gooley PR (2010) AMPK β subunits display isoform specific affinities for carbohydrates. FEBS letters, 584(15), 3499-3503.

Lennon JT, Muscarella ME, Placella SA, Lehmkuhl BK (2018) How, When, and Where Relic DNA Affects Microbial Diversity. mBio, 9(3), e00637-18. https://doi.org/10.1128/mBio.00637-18

Lim NY, Frostegard A, Vick SH, Bakken LR, Shapleigh JP (2020) Linking meta-omics to the kinetics of denitrification intermediates reveals pH-dependent causes of N2O emissions and nitrite accumulation in soil. *bioRxiv*.

Liu B, Frostegård Å, Bakken LR (2014) Impaired Reduction of $N_2O$ to $N_2$ in acid soils Is due to a posttranscriptional interference with the expression of *nosZ.* mBio 5(3):e01383-14. doi:10.1128/mBio.01383-14.

MacArthur PH, Shiva S, Gladwin MT (2007) Measurement of circulating nitrite and S-nitrosothiols by reductive chemiluminescence. J Chromatography B 851:93-105. https://doi.org/10.1016/j.jchromb.2006.12.012

Mallon CA, Le Roux X, Van Doorn GS, Dini-Andreote F, Poly F, Salles JF (2018) The impact of failure: unsuccessful bacterial invasions steer the soil microbial community away from the invader's niche. The ISME journal, 12(3), 728-741.

Mania D, Wolily K, Degefu T, Frostegård Å (2020) A common mechanism for efficient $N_2O$ reduction in diverse isolates of nodule-forming bradyrhizobia. Environmental Microbiology 22:17-31. https://doi.org/10.1111/1462-2920.14731

Molstad L, Dörsch P, Bakken LR (2007) Robotized incubation system for monitoring gases ($O_2$, NO, $N_2O$, $N_2$) in denitrifying cultures, Journal of microbiological methods 71:202-211

Molstad L, Dörsch P, Bakken LR (2016) Improved robotized incubation system for gas kinetics in batch cultures. Researchgate 2016, DOI: 10.13140/RG.2.2.30688.07680

Nadeem S, Bakken LR, Frostegård Å, Gaby JC, Dörsch P (2020) Contingent effects of liming on $N_2O$-emissions driven by autotrophic nitrification. Frontiers in Env Sci 598513 doi: 10.3389/fenvs.2020.598513

Nguyen TT, Myrold DD, Mueller RS (2019) Distributions of extracellular peptidases across prokaryotic genomes reflect phylogeny and habitat. Frontiers in microbiology, 10, 413.

Nielsen KM, Johnsen PJ, Bensasson D, Daffonchio D (2007) Release and persistence of extracellular DNA in the environment. *Environmental biosafety research*, *6*(1-2), 37-53.

Nilsen M, Madelen Saunders C, Angell IL, Arntzen MØ, Carlsen, KCL, Carlsen KH, ... Rudi K (2020) Butyrate levels in the transition from an infant-to an adult-like gut microbiota correlate with bacterial networks associated with eubacterium rectale and ruminococcus gnavus. *Genes*, *11*(11), 1245. https://doi.org/10.3390/genes11111245

Onaga S, Taira T (2008) A new type of plant chitinase containing LysM domains from a fern (Pteris ryukyuensis): Roles of LysM domains in chitin binding and antifungal activity, Glycobiology, Volume 18, Issue 5, Pages 414–423, https://doi.org/10.1093/glycob/cwn018

Parkin TB (1987) Soil microsites as a source of denitrification variability. Soil Sci Soc Am J 51:1194-1199

Parks DH, Imelfort M, Skennerton CT, Hugenholtz P, Tyson GW (2015) CheckM: assessing the quality of microbial genomes recovered from isolates, single cells, and metagenomes. Genome Res. 25: 1043 1055. doi:10.1101/gr.186072.114

Pasternak Z, Pietrokovski S, Rotem O, Gophna U, Lurie-Weinberger MN, Jurkevitch E (2013) By their genes ye shall know them: genomic signatures of predatory bacteria. *The ISME Journal*, *7*(4), 756-769.

Philippot L, Andert J, Jones CM, Bru D, Hallin S (2011) Importance of denitrifyers lacking the genes encoding the nitrous oxide reductase for $N_2O$ emissions from soil, Global Change Biology 17, 1494 – 1504.

Pinchbeck BJ, Soriano-Laguna MJ, Sullivan MJ, Luque-Almagro VM, Rowley G, Ferguson SJ, Roldán MD, Richardson DJ, Gates AJ (2019) A dual functional redox enzyme maturation protein for respiratory and assimilatory nitrate reductases in bacteria. Molecular microbiology 111(6), 1592–1603. https://doi.org/10.1111/mmi.14239

Pruesse E, Quast C, Knittel K, Fuchs BM, Ludwig W, Peplies J, Glöckner FO (2007) SILVA: a comprehensive online resource for quality checked and aligned ribosomal RNA sequence data compatible with ARB, *Nucleic acids research*, 35: 7188-96.

Raut P, Glass JB, Lieberman RL (2021) Archaeal roots of intramembrane aspartyl protease siblings signal peptide peptidase and presenilin. *Proteins: Structure, Function, and Bioinformatics*, *89*(2), 232-241.

Rawlings ND, Barrett AJ, Bateman A (2010) MEROPS: the peptidase database. *Nucleic acids research*, *38*(suppl_1), D227-D233. https://doi.org/10.1093/nar/gkp971

Robertson GP (2014) Soil Greenhouse Gas Emissions and Their Mitigation. Encycl Agric Food Syst, 5:185–196.

Rogelj J, Shindell D, Jiang K, Fifita S, Forster P, Ginzburg V, Handa C, Kheshgi H, Kobayashi S, Kriegler E, Mundaca L, Séférian R, Vilariño MV (2018) Mitigation pathways compatible with 1.5°C in the context of sustainable development. In: Global warming of 1.5°C. An IPCC Special Report on the impacts of global warming of 1.5°C above pre-industrial levels and related global greenhouse gas emission pathways, in the context of strengthening the global response to the threat of climate change, sustainable development, and efforts to eradicate poverty [Masson-Delmotte V, Zhai P, Pörtner HO, Roberts D, Skea J, Shukla PR, Pirani A, Moufouma-Okia W, Péan C, Pidcock R, Connors S, Matthews JBR, Chen Y, Zhou X, Gomis MI, Lonnoy E, Maycock T, Tignor M, Waterfield T (eds.)].In Press.

Russenes AL, Korsæth A, Bakken LR, Dörsch P (2016) Spatial variation in soil pH controls off-season $N_2O$ emission in an agricultural soil. Soil Biology and Biochemistry 99: 36-46

Rütting T, Boeckx P, Müller C, Klemedtsson L (2011) Assessment of the importance of dissimilatory nitrate reduction to ammonium for the terrestrial nitrogen cycle. Biogeosciences, 8(7), 1779-1791. https://doi.org/10.5194/bg-8-1779-2011

Schlüter S, Zawallich J, Vogel H-J, Dörsch P (2019) Physical constraints for respiration in microbial hotspots in soil and their importance for denitrification. Biogeosciences. 16. 3665-3678. 10.5194/bg-16-3665-2019.

Schulz-Bohm K, Martín-Sánchez L, Garbeva P (2017) Microbial Volatiles: Small Molecules with an Important Role in Intra- and Inter-Kingdom Interactions. Frontiers in microbiology, 8, 2484. https://doi.org/10.3389/fmicb.2017.02484

Sekar K, Linker SM, Nguyen J, Grünhagen A, Stocker R, Sauer U (2020) Bacterial glycogen provides short-term benefits in changing environments. Applied and environmental microbiology, 86(9).

Seemann T (2014) *Prokka: rapid prokaryotic genome annotation,* Bioinformatics 15;30(14):2068-9. PMID:24642063

Spiro S (2012) Nitrous oxide production and consumption: regulation of gene expression by gas-sensitive transcription factors. Philosophical Transactions of the Royal Society B: Biological Sciences, 367(1593), 1213-1225.

Thompson RL, Lassaletta L, Patra PK, Wilson C, Wells KC, Gressent A, Koffi EN, Chipperfield MP, Winiwarter W, Davidson EA, Canadell JG (2019) Acceleration of global N 2 O emissions seen from two decades of atmospheric inversion. *Nature Climate Change*, *9*(12), 993-998. Tian, H., Xu, R., Canadell, J.G. et al. (2020) A comprehensive quantification of global nitrous oxide sources and sinks. Nature **586,** 248–256. https://doi.org/10.1038/s41586-020-2780-0

Trujillo ME, Willems A, Abril A, Planchuelo AM, Rivas R, Ludena D, ... Velázquez E (2005) Nodulation of Lupinus albus by Strains of Ochrobactrum lupini sp. nov. Applied and Environmental Microbiology, 71(3), 1318-1327.

Wang Y, Guo J, Vogt RD, Mulder J, Wang J, Zhang X (2018) Soil pH as the chief modifier for regional nitrous oxide emissions: new evidence and implications for global estimates and mitigation. Global change biology, 24(2), e617-e626.Ward JH (1963) Hierarchical grouping to optimize an objective function, Journal of the American Statistical Association, 58, 236–244.

Waskom M et al (2020) Mvaskom/seaborn, Zendodo, DOI: 10.5281/zenodo.592845

Winiwarter W, Höglund-Isaksson L, Klimont Z, Schöpp W, Amann M (2018) Technical opportunities to reduce global anthropogenic emissions of nitrous oxide. Environ Res Lett, 13:014011.

Yu Y, Lee C, Kim J, Hwang S (2005) Group-specific primer and probe sets to detect methanogenic communities using quantitative real-time polymerase chain reaction. Biotechnol Bioeng 89(6), 670-679

Zhang H, Yohe, T, Huang, L, Entwistle S, Wu P, Yang, Z., Busk PK, Xu Y, Yin Y (2018) dbCAN2: a meta server for automated carbohydrate-active enzyme annotation. *Nucleic acids research*, *46*(W1), W95-W101. 10.1093/nar/gky418

Zumft WG (1997) Cell biology and molecular basis of denitrification. Microbiology Molecular Biology Review, 61, 553,536

Zurdo-Pineiro JL, Rivas R, Trujillo ME, Vizcaino N, Carrasco JA, Chamber M, ... Velazquez E (2007) Ochrobactrum cytisi sp. nov., isolated from nodules of Cytisus scoparius in Spain. International Journal of Systematic and Evolutionary Microbiology, 57(4), 784-788.